Phase plane Stäckel potential dynamics of the Manakov system

C. Polymilis,[1] K. Hizanidis,[2] and D. J. Frantzeskakis[1]
[1]Department of Physics, University of Athens, 157 84 Athens, Greece
[2]Department of Electrical and Computer Engineering, National Technical University of Athens, 157 73 Athens, Greece
(Received 19 September 1997)

A wide class of traveling-wave solutions of the Manakov system of coupled nonlinear Schrödinger equations is found to possess a potential which leads to separability in the Stäckel sense exhibiting two integrals of motion, which facilitates a thorough investigation of this system by nonlinear dynamics phase plane methods. On this basis, specific types of nonlinear waves are identified via a complete phase space trajectory investigation. The topological features of the phase space structure and the asymptotic behavior of the trajectory families involved are studied. Time domain analytical solutions are provided involving hyperelliptic integrals and their series expressions of the latter, in terms of the three elliptic integrals. Among the trajectory families, solitary-type envelope solutions to the Manakov system are easily identified on the basis of a limited number of parameters. [S1063-651X(98)07007-X]

PACS number(s): 03.40.Kf, 46.90.+s, 42.81.Dp, 42.65.Tg

I. INTRODUCTION

It is widely known that the system of two coupled nonlinear Schrödinger (NLS) equations, can be expressed in dimensionless form as follows:

$$i\,\frac{\partial u}{\partial \xi}=\frac{\partial^2 u}{\partial^2 \tau}+u(|u|^2+\sigma|v|^2), \tag{1a}$$

$$i\,\frac{\partial v}{\partial \xi}=\frac{\partial^2 v}{\partial^2 \tau}+v(|v|^2+\sigma|u|^2). \tag{1b}$$

In Eqs. (1a) and (1b), $u(\xi,\tau)$ and $v(\xi,\tau)$ are slowly varying envelopes, ξ and τ are normalized propagation distance and local time, respectively, while the coupling coefficient σ is the ratio between the cross- and self-phase modulation contributions to the nonlinear effects. For $6=1$, Eq. (1) is the so-called Manakov system.

This system can effectively describe the interaction of the envelopes of two carrier waves in dispersive media exhibiting a cubic nonlinearity and, therefore, it is (to some extent) universal from the point of view of its applications in physics. For example, it may effectively describe interactions among various wave modes in plasmas, ion-acoustic to Langmuir [1,2], or Langmuir to electromagnetic modes [3].

Especially, in the field of the nonlinear optics the following applications can be listed that are distinguished by the values of the coefficient σ: For $\sigma=0$, Eq. (1) represents a system of two uncoupled NLS equations, which govern the propagation of slowly varying electromagnetic waves in nonlinear optical fibers in the anomalous dispersion regime [4]. In this case, u (or v) represent the complex-valued pulselike envelope of the electric field distribution, ξ is the normalized spatial variable along the propagation distance and τ is the normalized time in the reference frame moving with the group velocity. For $\sigma\ll 1$, Eq. (1) governs the dynamics of the interaction of two modes in nonlinear optical fibers [5], or in directional couplers with weak intermodal coupling in the high-intensity limit [6,7]. In this case, u and v represent the complex valued envelopes of the two modes.

The system of Eqs. (1a) and (1b) governs also the interaction of two optical modes, u and v, through cross-phase modulation (CPM), or the interaction of two different polarizations, u and v, in single-mode birefringent optical fiber [8–10] in the limit where wave mixing is neglected (e.g., in the presence of rapid walkoff between the interacting modes). In this case, the coupling coefficient σ depends on the ellipticity of the fiber eigenmode, and in particular, $\sigma=2/3$ for linearly polarized modes, and, in the general case, $2/3\leqslant\sigma\leqslant 2$ for elliptical eigenmodes. The special value, $\sigma=1$, corresponds to at least two possible cases, namely the case of a purely electrostrictive nonlinearity [11,12] or, in the case of elliptical birefringence, when the angle between the major and the minor axes of the birefringence ellipse is approximately 35° [7]. Notice that for this value, $\sigma=1$, Eqs. (1a) and (1b) represent the so-called Manakov system [13], which is an integrable version of the system of two coupled NLS (CNLS) equations [14]. Actually, for $\sigma=0$ (uncoupled NLS) or $\sigma=1$ (Manakov equations) the system of Eqs. (1a) and (1b) admits soliton solutions that can be found by means of the inverse scattering method (ISM) [14,15].

The soliton solutions of the system, Eq. (1) (as well as of some generalized versions of it), has been the subject of increasing interest (see, for instance, [16]). This system with additional linear symmetric self-coupling terms has been studied by means of the quantum ISM [17], while, more recently, it was found that it can be transformed to the Manakov system, exhibiting thereby soliton solutions [18]. The system of two CNLS equations including nonintegrable terms has also been studied extensively. Exact vector soliton solutions of the CNLS equations with a birefringent term have been reported [19,20], while analytic solutions using a Lagrangian variational method have also been obtained [21,22]. Stability analyses have been performed [23–26] and there is also a large amount of numerical work [27–30]. Also, by using the ISM, a perturbed Manakov system [15] and a system of higher-order CNLS equations [31] have also been studied.

The dynamics of stationary-wave solutions of Eq. (1) can be studied by reducing this system to a Hamiltonian, one which is generally nonintegrable and only for some values of its parameters becomes integrable. Such Hamiltonian systems, leading to stationary-wave solutions of Eq. (1), have been studied numerically (nonintegrable cases). Some special solutions in closed form were found analytically (integrable cases) [32–34] as well.

On the other hand, it has been shown [35] that the multicomponent NLS can be reduced to an integrable infinite-dimensional Hamiltonian system by considering traveling-wave solutions to Eq. (1). However, solutions to this system have not been given in closed form although the corresponding integrals have been given as such. This is not surprising since it is well known in nonlinear dynamics of integrable Hamiltonian systems that in many cases, while the integrals of motion are known explicitly, the solutions to the dynamical equations have not been found in closed form: In general, finding the solutions of an integrable system is a nontrivial problem because it is directly connected with the determination of the so-called separability conditions. Specifically, there has been no systematic study to date of the dynamics of traveling-wave solutions of Eq. (1) along this line of reasoning. However, from the physics point of view, explicit knowledge of the solutions could be of great importance in many cases.

In this paper, a complete investigation of a wide class of traveling-wave solutions is made, by reducing the system in Eq. (1) to a Hamiltonian one. Specifically, Eq. (1) is reduced to a system of two coupled nonlinear ordinary differential equations. The latter represents a two-dimensional Hamiltonian system, which describes the motion of two coupled quartic anharmonic oscillators. As it will be shown, analytical results can be obtained only for $\sigma=1$, that is, for the Manakov system, since this is the only case in which the aforementioned dynamical system is integrable in the Liouville sense, exhibiting one integral besides the Hamiltonian. The second integral has been given explicitly in [36] but the solutions are not known in closed form. This system is shown to satisfy the Stäckel conditions. Thus it is separable in the Stäckel sense [37–39] and, therefore, its phase-space structure and asymptotic behavior (which incorporates solitary-type envelope solutions to the system of interacting waves) are identifiable on the basis of a limited number of parameters. The Stäckel character of a class of traveling-wave solutions of the Manakov system might possibly extend the applicability of these solutions to a wider class of physical problems: Stäckel potentials have been used extensively in the galactic dynamics where the construction of self-consistent models is mainstream research in this branch of physics [40,41], while the Manakov system mainly models nonlinear plasma and optical processes. We will find that, under certain well specified conditions, solitary structures may exist in the latter. Solitary structures also exist in the galactic dynamics. This underlying universality (from optics and plasmas to galaxies), a product of the same underlying (Hamiltonian) structure, is quite striking and, therefore, worth pursuing.

The traveling-wave solutions form a subspace of solutions for the Manakov system. This subspace is well defined since all periodic solutions are bounded. The solitary solutions are members of this subspace since they are the only asymptotic solutions corresponding to unstable periodic solutions (in the phase-space dynamical sense, not in the sense of the actual physical system they model): To each unstable periodic solution correspond two manifolds (one stable and one unstable) on which lie the asymptotic phase space trajectories. For the integrable case, which is going to be the focus of this work, the two manifolds coincide and their intersection with the Poincaré surfaces of section is the separatrices that correspond to the solitary solutions. However, under certain circumstances as we will see, the separatrices may separate periodic solutions from unbounded ones. The latter will have physical meaning only for the time scales (in the traveling-wave frame of reference) of applicability of Eq. (1), otherwise they cannot be considered as solutions to the Manakov system. The question about the magnitude of these time scales compared with the time scale of evolution of the particular physical system in hand is a very important, though open, question. This work will be the basis of addressing this issue in a future work as well as for dynamically studying the general nonintegrable case ($\sigma\neq 1$). It is expected that the latter will probably exhibit chaotic behavior as well.

The paper is organized as follows. In Sec. II, the reduction of Eq. (1) to a system of two coupled nonlinear ordinary differential equations, the transformation, and the integration of the associated Hamiltonian system on the basis of Stäckel's method are presented; in the Appendix, the calculation of the hyperelliptic integrals involved is outlined. In Sec. III the utilization of the Stäckel theorem leading to the separability of the system as well as the solutions are presented. The domains of motion and the topological structure of the Poincaré surfaces of section of the resulting Hamiltonian system are investigated in Sec. IV. In this section the character (elliptic or hyperbolic) of the periodic orbits (corresponding to the nonlinear traveling-wave solution), as well as the stability issue associated with it, are analyzed in terms of a few basic parameters of the physical system in hand. Solitary type asymptotic solutions are also identified. Finally, in Sec. V the main conclusions are recapitulated.

II. DYNAMICAL ANALYSIS

The main idea of the dynamical analysis is to consider traveling-wave solutions of Eq. (1) having the form

$$u(\xi,\tau)=2x(s)\exp[i(\lambda_1\xi-\mu\tau/2)], \tag{2a}$$

$$v(\xi,\tau)=2y(s)\exp[i(\lambda_2\xi-\mu\tau/2)]. \tag{2b}$$

In Eq. (2), $x(s)$ and $y(s)$ are unknown envelope functions (assumed to be real), which depend on the traveling-wave coordinate s. The physical significance of the arbitrary parameters μ, λ_1, and λ_2 is the following [42]: The parameter μ represents a shift of the frequency and is also related to the shift of the group velocity of the waves. The parameters λ_1 and λ_2, on the other hand, are related to the shifts of the wave numbers of the waves. They cannot be simultaneously eliminated by any suitable transformation to a moving frame of reference: Although the system, Eq. (1), is invariant under Galilean transformation [43], it can easily be shown, for example, that a choice for the velocity of the moving frame, U_0, that eliminates λ_1 (namely $U_0=\mu/2\lambda_1$) renders the new value of λ_2 equal to $\lambda_2-\lambda_1$. Notice that $\mu=0$ implies that the velocity of the wave is equal to the group velocity, the shifts of the wave numbers of u and v are equal to λ_1 and λ_2, respectively, and the trial solutions, Eq. (2), correspond to stationary waves. As is shown in [42], it is also possible to connect these parameters with the initial conditions (that is, with the initial information carried by the two interacting modes) required to be a certain type (envelope, frequency, and wave number) of nonlinear mode initially launchable.

Upon substituting Eq. (2) into Eq. (1), the following nonlinear coupled ordinary differential equations can be obtained:

$$\ddot{x}+(\lambda_1-\mu^2/4)x+4x(x^2+\sigma y^2)=0, \tag{3a}$$

$$\ddot{y}+(\lambda_2-\mu^2/4)y+4y(y^2+\sigma x^2)=0, \tag{3b}$$

where the notation $\dot{x}=dx/ds$, $\ddot{x}=d^2x/ds^2$, $\dot{y}=dy/ds$, $\ddot{y}=d^2y/ds^2$ has been introduced. These equations describe the motion of a particle in a two-dimensional central potential $V(x,y)$. The first integral of motion, namely the Hamiltonian function, has the form

$$H(x,y,\dot{x},\dot{y})=\tfrac{1}{2}(\dot{x}^2+\dot{y}^2)+V(x,y) \tag{4}$$

while the potential $V(x,y)$ is given by

$$V(x,y)=Ax^2+By^2+(x^2+y^2)^2+2(\sigma-1)x^2y^2, \tag{5}$$

where

$$A=\tfrac{1}{2}(\lambda_1-\mu^2/4), \quad B=\tfrac{1}{2}(\lambda_2-\mu^2/4). \tag{6}$$

The dynamical system represented by Eqs. (4) and (5) describes the motion of two coupled quartic anharmonic oscillators. The case $A=B$ (that is, $\lambda_1=\lambda_2$) corresponds to equal shifts (leading to zero shifts under a proper Galilean transformation) in the wave numbers of the two waves. In this case, the system is separable in parabolic coordinates and it has been studied in the literature [44].

This system is integrable only for $\sigma=1$ [which means that the original system, Eq. (1), is reduced to the Manakov system], exhibiting a second integral of motion [36]. The Hamiltonian function of the integrable case,

$$H(x,y,\dot{x},\dot{y})=\tfrac{1}{2}(\dot{x}^2+\dot{y}^2)+Ax^2+By^2+(x^2+y^2)^2, \tag{7}$$

is the first integral of motion while a second one exists, namely,

$$I(x,y,\dot{x},\dot{y})=(x\dot{y}-y\dot{x})^2+(B-A)(\dot{x}^2+2x^4+2x^2y^2+2Ax^2). \tag{8}$$

Both constants of the motion, $H(x,y,\dot{x},\dot{y})$ and $I(x,y,\dot{x},\dot{y})$, are merely fourth- and second-order polynomials of the amplitudes $(|u|,|v|)$ of the wave envelopes and their (slow) rates of change $(d|u|/ds,d|v|/ds)$ in the moving frame of reference, respectively. They are, therefore, closely connected with the local (in the moving frame) spectral energy density and the rate of slow variations of the latter; however, more precise physical interpretations are lacking. In the following, their arithmetic values, especially those of the Hamiltonian function, will be merely considered as reflecting the variation of the spectral energy density of the interacting nonlinear waves.

The overall problem of separability of the Hamiltonian function lies in the potential function $V(x,y)$. As we will see, this function is separable in elliptic coordinates. Then the Stäckel procedure [37–39] can be applied which will lead us to a special type of separability of equations of motion as we will see in the next section. The elliptic coordinates Q_1 and Q_2 (with the convention $Q_2<Q_1$, without loss of generality) are defined as the two roots at the equation,

$$\frac{x^2}{Q}+\frac{y^2}{Q-C}=1. \tag{9}$$

The real constant C plays only an auxiliary role and will relate back to the parameters A and B that enter in the potential function $V(x,y)$. Since the Cartesian coordinates (x,y) can be expressed with respect to (Q_1,Q_2) via the relations

$$x^2=\frac{Q_1Q_2}{C}, \quad y^2=\frac{(Q_1-C)(C-Q_2)}{C}, \tag{10}$$

there follows a restriction imposed on Q's (two alternatives for $C>0$ and $C<0$, respectively),

$$Q_1>0>Q_2>C \quad \text{or} \quad Q_1>C>Q_2>0. \tag{11}$$

The value of C can now be set via the following procedure: By differentiating Eq. (10) one readily yields for $\dot{x}$ and $\dot{y}$

$$\dot{x}=\frac{x}{2}\left(\frac{\dot{Q}_2}{Q_1}+\frac{\dot{Q}_2}{Q_2}\right), \quad \dot{y}=\frac{y}{2}\left(\frac{\dot{Q}_1}{Q_1-C}+\frac{\dot{Q}_2}{Q_2-C}\right). \tag{12}$$

The generating function that yields Eq. (12) (i.e., $\dot{x}=\partial F/\partial x$, $\dot{y}=\partial F/\partial y$) as well as the conjugate to Q_1 and Q_2 moments P_1 and P_2, respectively (i.e., $P_1=-\partial F/\partial Q_1$, $P_2=-\partial F/\partial Q_2$), can readily be found,

$$F=\frac{x^2}{4}\left(\frac{\dot{Q}_1}{Q_1}+\frac{\dot{Q}_2}{Q_2}\right)+\frac{y^2}{4}\left(\frac{\dot{Q}_1}{Q_1-C}+\frac{\dot{Q}_2}{Q_2-C}\right). \tag{13}$$

Upon evaluating P_1 and P_2, one can recast $\dot{Q}_1$ and $\dot{Q}_2$ in terms of the new coordinates and moment, by inverting the respective expression,

$$\dot{Q}_1=\frac{4P_1Q_1(Q_1-C)}{Q_1-Q_2}, \quad \dot{Q}_2=\frac{4P_2Q_2(c-Q_2)}{Q_1-Q_2}. \tag{14}$$

The Hamiltonian function, Eq. (7), now becomes, via Eqs. (10), (12), and (14),

$$H(Q_1,Q_2,P_1,P_2)=\{2P_1^2Q_1(Q_1-C)-2P_2^2Q_2(Q_2-C)+(Q_1+Q_2-C)^2(Q_1-Q_2)+[AQ_1Q_2+B(Q_1-C)(C-Q_2)](Q_1-Q_2)C^{-1}\}(Q_1-Q_2)^{-1}. \tag{15}$$

By choosing the parameter C such that

$$C=B-A, \tag{16}$$

the numerator of the expression Eq. (15) becomes separable, i.e., it can then be written as the algebraic sum of two expressions, each one involving only one conjugate pair. In other words, the new Hamiltonian function becomes

$$H(Q_1,Q_2,B_1,B_2)=\frac{\sum_{j=1}^{2}(-1)^{3-j}Q_j(Q_j-C)(2P_j^2+Q_j+A)}{Q_1-Q_2}. \tag{17}$$

It is worth noticing that, in its new description, the Hamiltonian [Eq. (17)], being quadratic in Q, retains its initial (weak) interpretation as a measure of the variation of the spectral energy density, since products of Q's are quadratically related to squares of the envelope amplitudes [Eq. (10)].

The second integral, $I(Q_1,Q_2,P_1,P_2)$, Eq. (8), can also be expressed in terms of the new canonical pairs. Utilizing Eqs. (10), (12), and (14) as well as the expression for the new Hamiltonian function, Eq. (17) in Eq. (8) yields

$$I(Q_1,Q_2,P_1,P_2)=Q_i[H(Q_1,Q_2,P_1,P_2)-(Q_i-C)(2P_i^2+Q_i+A)],\quad i=1,2. \tag{18}$$

III. SEPARABILITY OF THE SYSTEM AND SOLUTIONS

The dynamical system at hand in its new description, Eq. (17) can be made separable in the Stäckel sense. In addition, using the expression for the second integral, Eq. (18), we are able to obtain the solutions of the system at hand in closed form. The utilization of Stäckel's theorem allows us to reach an equation that involves the following: The generalized coordinates Q_1 and Q_2, the pair (h,i) of values for the respective generalized Hamiltonian, and the second integral of motion as well as the coordinates of reference $Q_1(s_0)$ and $Q_2(s_0)$. According to Stäckel, one may introduce a potential function $U(Q_1,Q_2)$ such that

$$P_j=\frac{\partial U}{\partial Q_j},\quad j=1,2 \tag{19}$$

for *fixed values* for the respective Hamiltonian $h=H(Q_1,Q_2,\partial U/\partial Q_1,\partial U/\partial Q_2)$ and the second invariant function $i=I(Q_1,Q_2,\partial U/\partial Q_1,\partial U/\partial Q_2)$ (lower case denotes fixed values for the respective functions). Equation (18) then yields

$$P_j=(-1)^{3-j}\left(\frac{Q_j[h-(Q_j+A)(Q_j-C)]-i/2}{2Q_j(Q_j-C)}\right)^{1/2},\quad j=1,2. \tag{20}$$

One can, therefore, deduce that $U(Q_1,Q_2)$ can be expressed as a sum of two potential functions (each being depended only upon a single generalized coordinate, namely, the functions) $U^{(j)}(Q_j)$ with $j=1,2$. Thus, Eq. (20) can be rewritten as follows:

$$\frac{dU^{(j)}}{dQ_j}=(-1)^{3-j}\left(\frac{Q_j[h-(Q_j+A)(Q_j-C)]-i/2}{2Q_j(Q_j-C)}\right)^{1/2},\quad j=1,2. \tag{21}$$

By integrating Eq. (21), the value of the potential function $U(Q_1,Q_2)$ (apart of an arbitrary constant) can readily be obtained,

$$U(Q_1,Q_2;h,i)=\sum_{j=1}^{2}(-1)^{3-j}\int^{Q_j}dQ_j'\left(\frac{Q_j'[h-(Q_j'+A)(Q_j'-C)]-i/2}{2Q_j'(Q_j'-C)}\right)^{1/2}. \tag{22}$$

Following Stäckel, one has

$$d\,\frac{\partial U}{\partial Q_{j0}}=-\frac{\partial H}{\partial Q_{j0}}\,ds, \tag{23}$$

where Q_{j0} plays the role of the initial canonical coordinates. Combining now Eqs. (22) and (23) readily yields

$$ds\sqrt{8}=\sum_{j=1}^{2}dQ_j(-1)^j\left(\frac{Q_j}{(Q_j-C)\{Q_j[h-(Q_j+A)(Q_j-C)]-i/2\}}\right)^{1/2}. \tag{24}$$

This expression can be integrated providing the temporal structure of an orbit on the planar subspace (Q_1,Q_2), namely an expression of the type $f(Q_1,Q_2;s;Q_{10},Q_{20};h,i)=0$. However, the evaluation of a such a function is confronted with expressing the hyperelliptic integrals [45] involved in the RHS of Eq. (24) in terms of known functions.

In order to integrate Eq. (24), knowledge of the domain of variation of Q_1 and Q_2 is necessary. It should be emphasized that the term ''domain'' refers to a specified orbit in phase space, that is, the Hamiltonian and the second invariant are considered as fixed with values h and i, respectively.

In addition to the restriction originating from the coordinate transformation, Eq. (11), a real solution of Eq. (24) in the time domain imposes the following additional requirement:

$$Q_j(Q_j-C)\{i/2+Q_j[(Q_j+A)(Q_j-C)-h]\}\leqslant 0, \quad j=1,2. \tag{25}$$

As far as the cubic polynomial within the curly brackets is concerned, there exist two cases to be examined: the case where there is only one real root, $Q^{(1)}$, and the case of three real roots, $Q^{(1)}<Q^{(2)}<Q^{(3)}$. For the first case it is readily evident [by utilizing Eq. (11)] that, independently of C, Eq. (25) cannot be satisfied. In the second case, also independently of C, one obtains the following condition:

$$Q^{(1)}<Q_2<Q^{(2)}<Q_1<Q^{(3)}, \tag{26}$$

that is, an important physical result is obtained: the domains of the values of Q_1 and Q_2 are disjoint and bounded by the (always) real roots of the aforementioned cubic polynomial. Therefore, the envelope values of the traveling-wave solutions (directly associated to Q's via the elliptic transformation) exhibit the fundamental property that certain functions of them (namely the Q's) can be initially launched independently inside predefined domains depended upon the desired spectral characteristics. We will return to this subject in the next section in detail.

The pair of values of the two constants of the motion obviously provides a certain orbit that passes through the reference position at $s=s_0$. Integration of Eq. (24) yields

$$\sqrt{8}(s-s_0)=-\int_{Q_1(s_0)}^{Q_1(s)}\frac{dx\sqrt{x}}{\sqrt{(x-C)\{x[h-(x+A)(x-C)]-i/2\}}}+\int_{Q_2(s_0)}^{Q_2(s)}\frac{dx\sqrt{x}}{\sqrt{(x-C)\{x[h-(x+A)(x-C)]-i/2\}}}. \tag{27}$$

It can be easily seen by utilizing the results in the Appendix that, depending upon C, Eq. (27) yields the following converging series.

For $C<0$, $1\geqslant -Q_1/C$,

$$s-s_0=\frac{1}{\sqrt{8|C|}}\sum_{i=0}^{\infty}\left(\frac{1}{4}\right)^i\frac{(2i)!}{(i!)^2(2i-1)}\left[I_i^{(1)}\left(\frac{1}{1-\frac{Q_1(s)}{C}}\right)-I_i^{(1)}\left(\frac{1}{1-\frac{Q_1(s_0)}{C}}\right)+I_i^{(3)}\left(1-\frac{Q_2(s)}{C}\right)-I_i^{(3)}\left(1-\frac{Q_2(s_0)}{C}\right)\right]. \tag{28a}$$

For $C<0$, $-Q_1/C\geqslant 1$,

$$s-s_0=\frac{1}{\sqrt{8|C|}}\sum_{i=0}^{\infty}\left(\frac{1}{4}\right)^i\frac{(2i)!}{(i!)^2(2i-1)}\left[(-1)^iI_i^{(2)}\left(-\frac{C}{Q_1(s)}\right)-(-1)^i-I_i^{(2)}\left(-\frac{C}{Q_1(s_0)}\right)+I_i^{(3)}\left(1-\frac{Q_2(s)}{C}\right)-I_i^{(3)}\left(1-\frac{Q_2(s_0)}{C}\right)\right]. \tag{28b}$$

For $C>0$,

$$s-s_0=-\frac{1}{\sqrt{8|C|}}\sum_{i=0}^{\infty}\left(\frac{1}{4}\right)^i\frac{(2i)!}{(i!)^2}\left[I_i^{(4)}\left(-\frac{C}{Q_1(s)}\right)-I_i^{(4)}\left(\frac{C}{Q_1(s_0)}\right)+\frac{1}{2i-1}I_i^{(5)}\left(1-\frac{Q_2(s)}{C}\right)-\frac{1}{2i-1}I_i^{5}\left(1-\frac{Q_2(s_0)}{C}\right)\right], \tag{28c}$$

where the functions $I_i^{(\gamma)}$ are connected through recurrence relations to three basic functions of the same argument, namely, $I_{-1}^{(\gamma)}$, $I_0^{(\gamma)}$, and $I_1^{(\gamma)}$. The latter, in turn, are directly related to the elliptic integrals of the first, second, and third kind (see the Appendix). The superscript $\gamma=1,2,...,5$ refers to five distinct recurrence relations.

Equations (28) provide the orbits in the generalized configuration space Q_1-Q_2. However, the temporal connection between these two dynamical variables is only indirectly provided by these equations since only the time variable can explicitly be expressed in terms of a series of functions of Q_1 and Q_2 and not vice versa. There exists a remote possibility, Eq. (28), to be invertible, though the inversion seems an extremely arduous task and goes beyond the scope of this work. Instead, it is highly important to investigate the possibility of the quasiperiodic behavior of Q_1 and Q_2, as well as the existence of nondegenerate bounded asymptotic states (that is, states of vanishing nonlinear frequency that acquire finite Q's and P's). The latter correspond to *solitary envelope solutions* $x(s)$ and $y(s)$ of the problem at hand. The study can be facilitated by investigating the structure of the phase space considering a Poincaré surface of section.

IV. POINCARÉ SURFACE OF SECTION. DOMAINS OF MOTION AND TOPOLOGY

The study of the dynamics of the Hamiltonian system at hand [in terms of the second integral, Eq. (18)] is highly facilitated by studying the topological features of the sets of points of successive intersections of a trajectory with a two-dimensional surface in the phase space. On such a surface of section [either (Q_1,P_1) or (Q_2,P_2)], the so-called Poincaré surface of section, a trajectory of fixed Hamiltonian value provides a set of points of intersection that forms an invariant curve. Each invariant curve corresponds to a different value of the second integral and represents a quasiperiodic orbit located on a two-dimensional torus and is also confined on the surface $H(Q_1,Q_2,P_1,P_2)=h$ of the four-dimensional phase space. In this space, it is well known that the invariant curves are the intersections of the two-dimensional tori with the surface of section. According to the Kolmogorov-Arnold-Moser (KAM) theorem, and since the system is integrable, for the *same* arithmetic value of the energy the set of the tori is continuous and thus the invariant curves, corresponding to *different* arithmetic values of the second integral, are continuously distributed on the surface of section.

Of special interest are the invariant points that represent periodic orbits on a Poincaré surface of section. On the surface of section the location of the periodic orbits of an integrable system can be found in terms of the second integral [46], by setting

$$\frac{\partial I}{\partial Q_j}=\frac{\partial I}{\partial P_j}=0. \tag{29}$$

Solving Eq. (29) leads to a set of points $(Q_j,P_j;\ j=1$ or $2)$ on the respective Poincaré surfaces of section [on (Q_1,P_1) or (Q_2,P_2) planes], which correspond to periodic orbits. On the other hand, depending upon the sign of the quantity

$$\Delta\equiv\frac{\partial^2 I}{\partial Q_j^2}\frac{\partial^2 I}{\partial P_j^2}-\left(\frac{\partial^2 I}{\partial Q_j\partial P_j}\right)^2,\quad j=1\ \text{or}\ 2, \tag{30}$$

where the derivatives are taken at the solution of Eq. (29), the corresponding periodic orbits are characterized as stable ($\Delta>0$, i.e., elliptic points) or as unstable ($\Delta<0$, i.e., hyperbolic points). For the Hamiltonian system at hand, we find the periodic orbits by using the second integral (18). Then solving Eq. (29), the periodic orbits solutions are six in general,

$$Q_j=0,\ \ P_j=\pm(Q_+Q_-/2C)^{1/2}, \tag{31a}$$

$$Q_j=C,\ \ P_j=\pm\{[C(2Q_--3C)-Q_+(Q_--2C)]/2C\}^{1/2}, \tag{31b}$$

$$Q_j=Q_1^{(\pm)},\qquad P_j=0, \tag{31c}$$

where $Q_1^{(\pm)}$ are given by

$$Q_1^{(\pm)}\equiv\frac{Q_++Q_-\pm(Q_+^2+Q_-^2-Q_+Q_-)^{1/2}}{3} \tag{32}$$

and $Q\pm$ are parameters, functions of h, A, and B, given by

$$Q_\pm\equiv-A+\frac{B}{2}\pm\left(\frac{B^2}{4}+h\right)^{1/2}. \tag{33}$$

It is straightforward, though lengthy, to show that the first and the second pair of periodic orbits in Eq. (31) (when they possess real-valued generalized momenta) always correspond to unstable periodic orbits (hyperbolic points on the respective Poincaré surface of section). As far as the third pair is concerned, it corresponds to stable periodic orbits (elliptic points) as long as the following condition is satisfied:

$$\pm Q_1^{(\pm)}(Q_1^{(\pm)}-C)^{1/2}>0. \tag{34}$$

The elliptic and the hyperbolic points will be called, respectively, ○ points and × points thereafter ($j=1$ or 2).

A. The character of the periodic orbits and the parameter space

It is well known from the basic theory of the dynamical systems that the separatrices separate regions of qualitatively different types of motion. As far as the stationary or traveling-wave solutions of the NLS are concerned, it is also well known that separatrices correspond to a *solitary type* of solution: Asymptotic states of periodic (in the traveling-wave coordinate s) nonlinear waves of infinite period [47]. Such types of solutions in the problem at hand will be of paramount importance: In wave-related applications, for example (such as in optics), the solitary nature of the envelope solutions to Eq. (1) will assure the possibility of modulated pulse propagation in the associated medium, and so on.

The topological features of the aforementioned separatrices are tightly connected with the position and the number of the × points, which the particular choice of the parameters A, B, and h allows. It was already mentioned in the preceding section that the two pairs of points defined by Eq. (31) are always (when they do exist) × points lying on the lines $Q_i=0$ and $Q_i=C$. The character of the third pair depends upon the choice of the parameters A, B, and h. As we already mentioned in the preceding sections, the latter set of parameters is directly related with shifts in the wave numbers and frequencies as well as the spectral energy density variation of the interacting waves. In order to investigate the existence and the character of all × and ○ points involved in the topological structure of the Poincaré surfaces of sections, a very informative and comprehensive view of the structure and the respective dynamical behavior is devised based on this particular set of parameters.

One can construct for a specified value of the Hamiltonian, h, a chart on the (A,B)-parameter plane (Figs. 1 and 2). On each such chart there exists a network of curves $f(A,B;h)=0$, which divide the parameter space into several subspaces corresponding to a different character of the third pair of the periodic orbits $Q_j=Q_1^{(\pm)}$, $P_j=0$ (××, ○○, ×○, and ○× with the first character symbol referring to Q_1^- and the second to Q_1^+). The several levels of shading refer to the status (existence or no existence) of the first two pairs of Eq. (31). Figures 1 and 2 refer to the respective cases of positive and negative Hamiltonian values, h.

For the case $h>0$ ($h=4$ in the example shown) there exist sixteen subregions. The network of borderlines of these subregions consists of the curves $A=B$, $A=B/2$, $A=2B$, $h=B(B-A)$, and $h=A(A-B)$. The subregions, which are white, refer to a choice in (A,B) that allows only the third pair [given by Eq. (31c)] of periodic orbits to exist. These

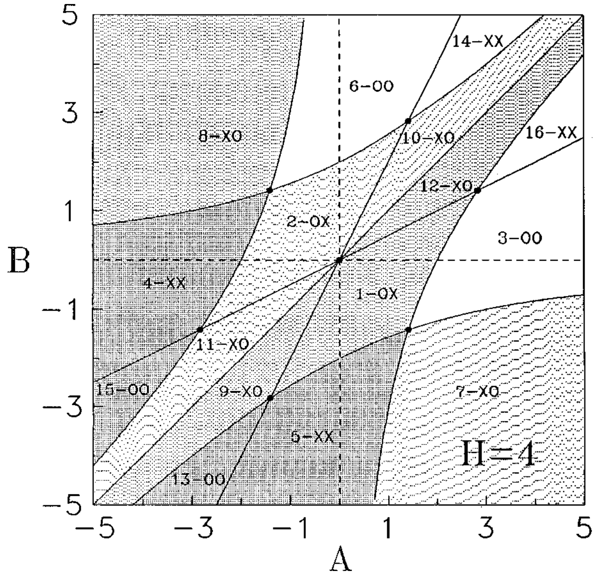

FIG. 1. (A,B)-parameter space for $h=4$. The character of the third pair of periodic orbits is indicated [with the first (second) character symbol referring to $Q=Q_1^-$ $(Q=Q_1^+)$] along with the status of the first two pairs (always hyperbolic) in the sixteen subregions: White, only the third pair exists; light gray, only the second and the third pairs exist; gray, only the first and the third pairs exist; dark gray, all three pairs of periodic orbits exist.

orbits are both elliptic (subregions 3 and 6) or both hyperbolic (subregions 14 and 16) in character. In the light-gray subregions (totally four subregions: 2, 7, 10, and 11) only the second and the third pair of periodic orbits exist [Eq. (31b) and (31c)]. The character of the third pair is mixed (one hyperbolic and one elliptic). Symmetrically to the previous set of subregions (with respect to the $A=B$ axis of symmetry) lie four subregions indicated by a gray color (1, 8, 9, and 12). In these subregions only the first and the third pairs exist. The latter corresponds to orbits of opposite character, as before. In the remaining four subregions, indicated by a dark-gray color, all three pairs of periodic orbits exist and both orbits of the third pair have the same character: hyperbolic in 4 and 5 and elliptic in 13 and 15.

For the case $h<0$ ($h=-2$ in the example shown), on the other hand, there exist six subregions. The respective network of borderlines are the curves $h=B(B-A)$, $h=A(A-B)$, $A=B$, $A=-2|H|^{1/2}$, and $B=-2|H|^{1/2}$. In the white quadrant to the left and above the latter two lines, respectively, there exist no choices in the parameter values A and B that render physically meaningful x's and y's [that is, a non-negative value of the ''kinetic energy'' $h-V(x,y)$]. In the two light-gray subregions (2 and 4) only the second and the third pair of periodic orbits exist [Eq. (31b) and (31c)] and the character of the third pair is mixed (one hyperbolic and one elliptic). Symmetrically to the previous set of subregions (with respect to the $A=B$ axis of symmetry) lie two subregions indicated by a gray color (1 and 3). In these subregions only the first and the third pairs exist. The latter corresponds to orbits of opposite character, as before. In the remaining two subregions 5 and 6, indicated by a dark-gray color, all three pairs of periodic orbits exist and both orbits of the third pair are elliptic.

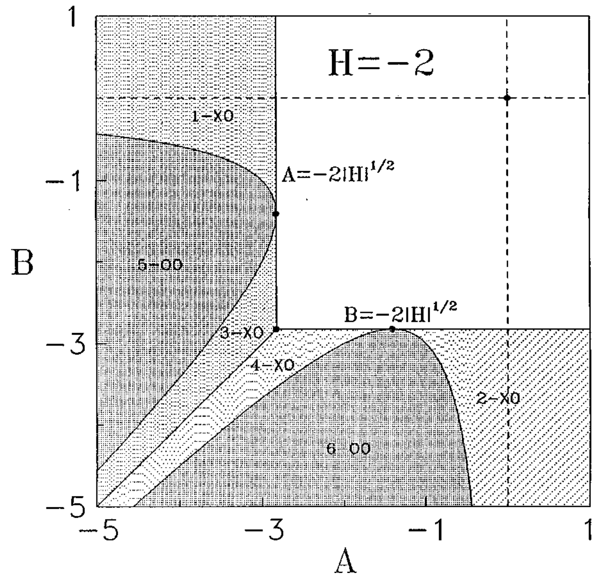

FIG. 2. (A,B)-parameter space for $h=-2$. The character of the third pair of periodic orbits is indicated [with the first (second) character symbol referring to $Q=Q_1^-$ $(Q=Q_1^+)$] along with the status of the first two pairs (always hyperbolic) in the six subregions: Light gray, only the second and the third pairs exist; gray, only the first and the third pairs exist; dark gray, all three pairs of periodic orbits exist; white, there exist no choices in the parameter values A and B that render a non-negative value of the ''kinetic energy'' $h-V(x,y)$.

B. Structure of the phase space

The *permissible* region of motion in the phase space is defined via the requirement of the ''kinetic energy'' part of

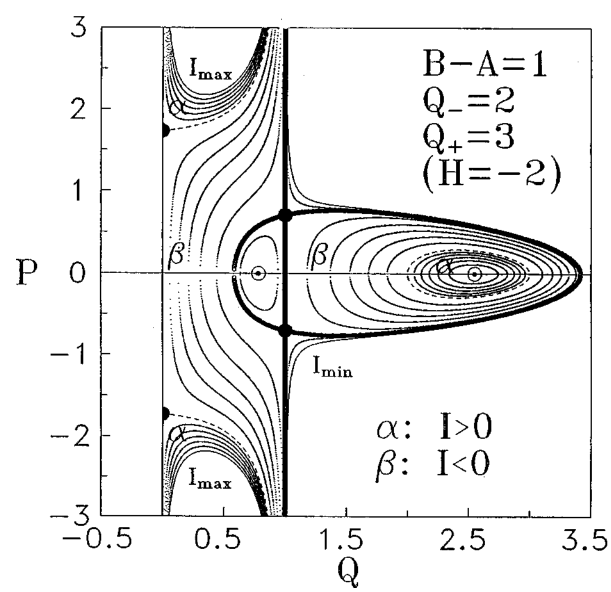

FIG. 3. Poincaré surface of section for a case with $[C<Q_-<Q_+,\ Q_1^{(-)}<C]$. The dashed curves correspond to the contour $i=0$. The thick solid curves are the separatrices. The vertical one coincides with the line $Q=C$. The elliptic and the hyperbolic points are denoted, respectively, by a circle and a thick dot. Contours of constant value of the second invariant, I, are shown.

the Hamiltonian function being non-negative. For a fixed value of the Hamiltonian, h (that is, for a fixed envelope amplitude variation), this requirement, expressed in terms of the coordinates Q_1 and Q_2, can be shown that it leads to the following:

$$\text{at } P_i=0: Q_2^{(-)}<Q_i<Q_2^{(+)}, \quad i=1,2, \tag{35}$$

where the parameters $Q_2^{\pm}$ are defined by

$$Q_2^{\pm}\equiv\frac{Q_++Q_-\pm 2(Q_+^2+Q_-^2-Q_+Q_-)^{1/2}}{3}, \tag{36}$$

where $Q_\pm$ are given by Eqs. (33). This means that for a given arithmetic value h of the Hamiltonian, the topological structure of the invariant curves inside the permissible region of motion depends upon the ordering of the parameters $Q_\pm$ and C and, occasionally, upon the ordering of the parameter $Q_1^{(-)}$ and C.

We find seven topologically distinct cases by using the condition (35) and Eqs. (32), (33), and (36). These cases are respectively shown:

$$1:\quad 0<C<Q_-<Q_+\ [1\text{a}:\quad Q_1^{(-)}<C,\ 1\text{b}:\quad C<Q_1^{(-)}];\ 2:\quad C<0<Q_-<Q_+;\ 3:\quad C<Q_-<0<Q_+;$$
$$4:\quad 0<Q_-<C<Q_+;\ 5:\quad Q_-<C<0<Q_+\ [5\text{a}:\quad Q_1^{(-)}<C,\ 5\text{b}:\quad C<Q_1^{(-)}]. \tag{37}$$

We notice that for a given orbit in the phase space and for a given arithmetic value h of the Hamiltonian, the orbit intersections with the subspaces (Q_1,P_1) or (Q_2,P_2) are topologically identical. Therefore, it is sufficient to study only the various plane curves (Q_1,P_1) that correspond to different choices of the values of the Hamiltonian.

Choosing suitable values for the parameters h, A, and B, in Figs. 3–9 the corresponding Poincaré surface of section of the above seven distinct cases is shown. In all cases (37), once the set of parameter values is chosen the location and the stability character of the corresponding periodic are found, by using Eqs. (31), (32), (33), and the condition (34). The ○ points and × points are denoted by a circle and a thick dot, respectively.

The permissible region extends within the corresponding limiting curves. These curves, when they intersect the Q axis, do it at one or both points $Q=Q_2^{(\pm)}$. Also the limiting curves are invariant curves and thus they are calculated by using the form of the second invariant Eqs. (19). Calling the corresponding values of the second invariant $I_{\min}$ and $I_{\max}$, they are found as functions of the parameters A, B, and h. Their expressions in terms of $Q_\pm$ are

$$I_{\min}=\frac{2}{27}[Q_+^3+Q_-^3+(Q_+-Q_-)^3 -2(Q_+^2-Q_+Q_-+Q_-^2)^{3/2}], \tag{38a}$$

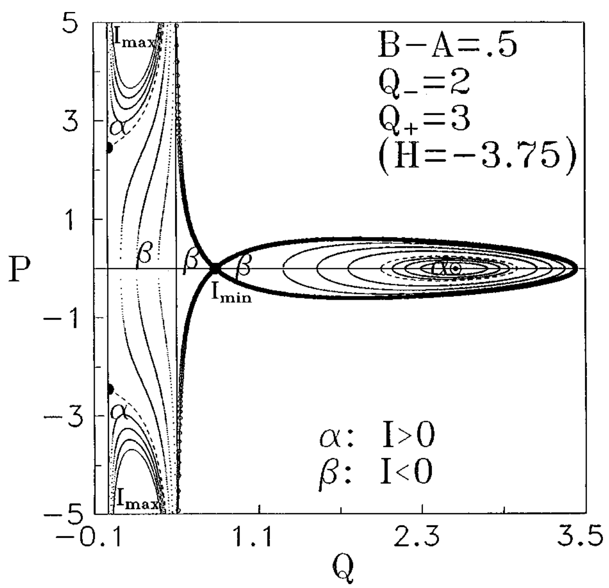

FIG. 4. Poincaré surface of section for a case with $[C<Q_-<Q_+,\ C<Q_1^{(-)}]$. The dashed curves correspond to the contour $i=0$. The thick solid curve is the separatrix, which, in this case coincides with the contour $i=I_{\min}$. The elliptic and the hyperbolic points are denoted, respectively, by a circle and a thick dot. Contours of constant value of the second invariant, I, are shown.

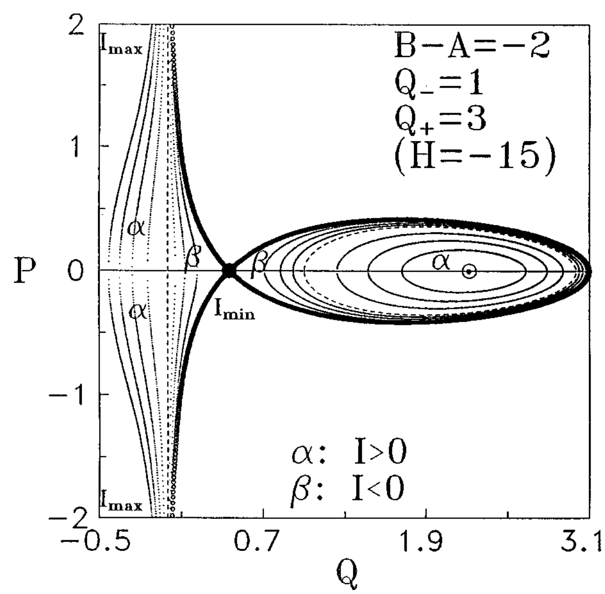

FIG. 5. Poincaré surface of section for a case with $C<0<Q_-<Q_+$. The dashed curve and vertical line correspond to the contour $i=0$. The thick solid curve is the separatrix, which, in this case, coincides with the contour $i=I_{\min}$. The sole elliptic and the hyperbolic points are denoted, respectively, by a circle and a thick dot. Contours of constant value of the second invariant, I, are shown.

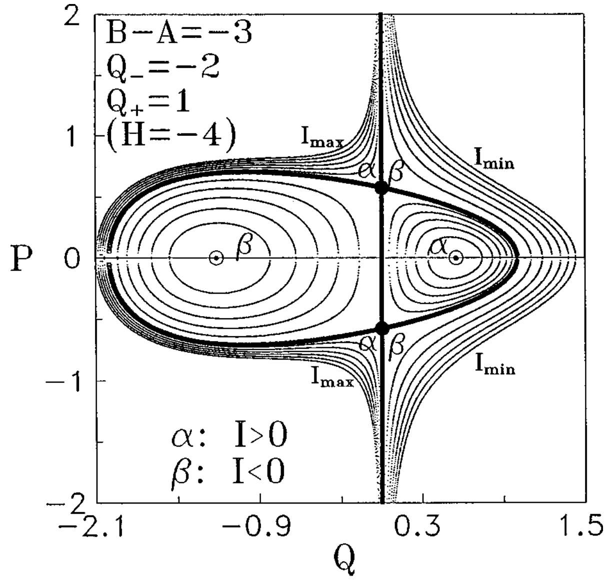

FIG. 6. Poincaré surface of section for a case with $C<Q_-<0<Q_+$. The thick solid curves are the separatrices, which, in this case, coached with the contour $i=0$. The elliptic and the hyperbolic points are denoted, respectively, by a circle and a thick dot. Contours of constant value of the second invariant, I, are shown.

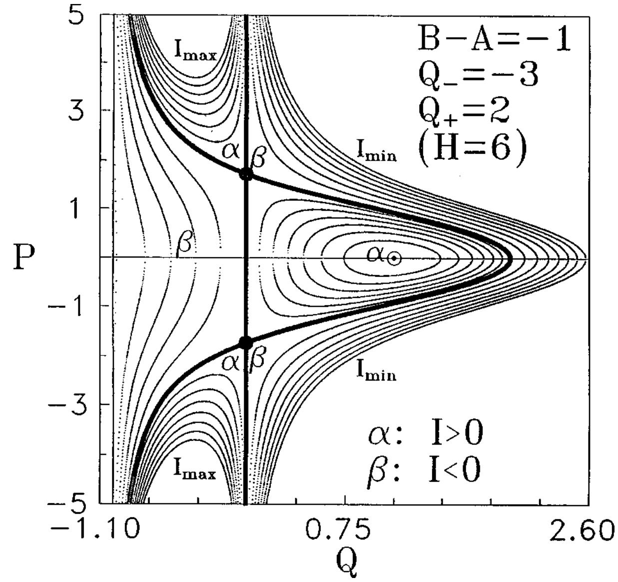

FIG. 8. Poincaré surface of section for a case with $[Q_-<C<0<Q_+,\ Q_1^{(-)}<C]$. The thick solid curves are the separatrices, which, in this case, coached with the contours of $i=0$. The elliptic and the hyperbolic points are denoted, respectively, by a circle and a thick dot. Contours of constant value of the second invariant, I, are shown.

$$I_{\max}=\frac{2}{27}\,[Q_+^3+Q_-^3+(Q_+-Q_-)^3+2(Q_+^2-Q_+Q_-+Q_-^2)^{3/2}]. \tag{38b}$$

The thick solid curves, in Figs. 3–9, correspond to separatrices that pass through the unstable periodic orbits (hyperbolic points on the surface of section). These separatrices correspond to the asymptotic solutions of the system and separate the phase space in regions of a different type of ''motion.'' We have also calculated many invariant curves. These curves represent quasiperiodic orbits and correspond to different arithmetic values I of the second invariant depending on the initial conditions. Thus the invariant curves

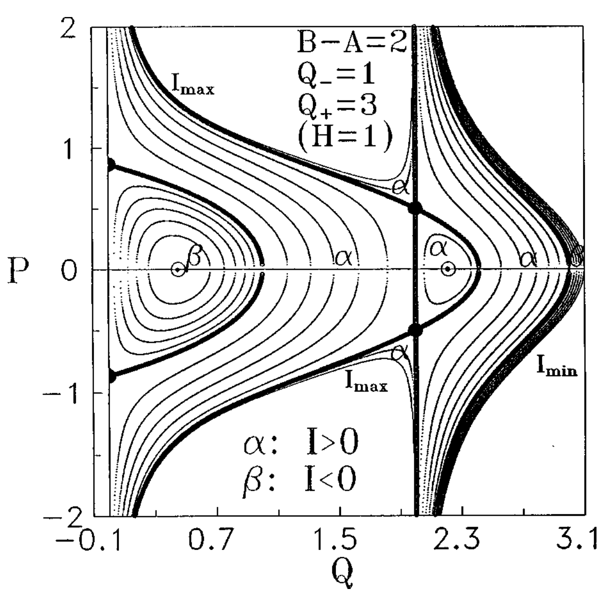

FIG. 7. Poincaré surface of section for a case with $0<Q_-<C<Q_+$. The thick solid curves, except for the rightmost one, are the separatrices. The leftmost one, along with the dashed curve in the right, are contours of $i=0$. The rightmost thick solid curve is also an $i=0$ contour. The elliptic and the hyperbolic points are denoted, respectively, by a circle and a thick dot. Contours of constant value of the second invariant, I, are shown.

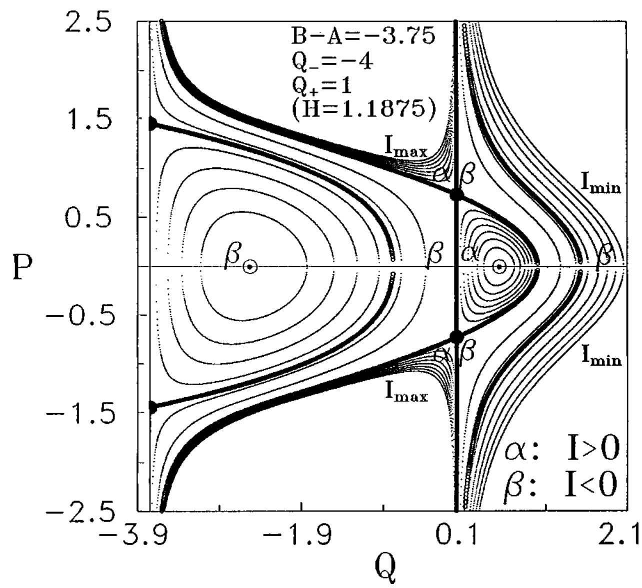

FIG. 9. Poincaré surface of section for a case with $[Q_-<C<0<Q_+,\ C<Q_1^{(-)}]$. The thick solid curves, except for the rightmost one, are the separatrices. The vertical line $Q=0$ (a separatrix) and the separatrix that intersects it coached, in this case, with the contour of $i=0$. The rightmost thick solid curve is also an $i=0$ contour. The elliptic and the hyperbolic points are denoted, respectively, by a circle and a thick dot. Contours of constant value of the second invariant, I, are shown.

are calculated, because the system is integrable, in terms of the second integral Eqs. (19) instead of the calculation of the orbits. The value of the second invariant can be positive or negative (namely, $i>0$ or $i<0$). The dashed lines and curves correspond to the contour $i=0$ whose intersection with the Q axis is one or both points $Q=Q_{\pm}$. We notice that the permissible region for the cases 1a, 1b, and 4 (Figs. 3, 4, and 7) is defined by the limiting curves and the line $Q=0$. The latter line becomes, instead, the line $Q=C$ for the cases 5a and 5b for Figs. 8 and 9.

It is now evident that all the information about the behavior of the system at hand can be obtained in an explicit way in terms of its second integral. In other words, for given values of the parameters A, B, and h (directly related to the spectral characteristics if one aims towards nonlinear optics applications, for example) a variety of quantities of great practical interest can then be easily evaluated or, at least, estimated: The set of the required initial conditions for launching, the boundaries of the envelope solution variations with s, and, most importantly, the kind of motion (solitary or otherwise) and the asymptotic solutions themselves as well.

C. Asymptotic solutions

The asymptotic solutions, corresponding to the separatrices, are of great physical importance since they represent generally solitary or/and soliton solutions. Thus a detailed discussion of the asymptotic solutions of the system at hand is needed.

All seven subcases (37) of the problem at hand, from the point of view of the form of the asymptotic states they possess, can be grouped into four distinct families that are summarized and tabulated in Fig. 10.

In the subcase 1a, illustrated in Fig. 3 ($0<C<Q_-<Q_+$ with $Q_1^{(-)}<C$), it is clear that there exists a pair of asymptotic trajectories in the phase space whose corresponding invariant curves on the surfaces of section are the thick solid curves passing through the pairs of the hyperbolic points lying on the lines $Q_1=C$, $Q_2=C$. Furthermore, they correspond to a *negative* value of the second invariant (subdomains β). The curved branches of these two asymptotic states coincide and are bounded. The respective vertical branches are complementary (one line segment between the two hyperbolic points and one pair of semi-infinite lines). They actually form a pair of identical sets of three line segments. The curved branches correspond to solitary envelope solutions of the physical system at hand. The two coinciding states ($Q_1=C$ and $Q_2=C$) on the two sets of vertical branches, on the other hand, are degenerate asymptotic states: In terms of the envelope functions [utilizing Eq. (10)] they correspond to the states $x(s)=\pm 1$ and $y(s)=0$.

One may observe a similar structure for the subcase illustrated in Fig. 6, namely, subcase 3 in Eq. (37): The pairs of hyperbolic points lie on the vertical lines $Q_1=0$, $Q_2=0$ and the two coinciding states ($Q_1=0$ and $Q_2=0$) on the respective sets of vertical branches are the degenerate ones, which, in this case, are the (identical) states $x(s)=0$ and $y(s)=0$. The value of the second invariant for the appearance of this solitary envelope solution is *zero* in this subcase.

The subcases that are illustrated in Figs. 4, 5, and 8 [subcases 1b, 2, and 5a in Eq. (37)] do not possess pairs of bounded asymptotic solutions: The bounded asymptotic state for Q_1 is accompanied by an unbounded (and nondegenerate) asymptotic one for Q_2 and vice versa. The respective values of the second invariant for the first two of these subcases are the *minimum* (and *negative*) ones. As far as the third subcase is concerned, the second invariant is *zero*.

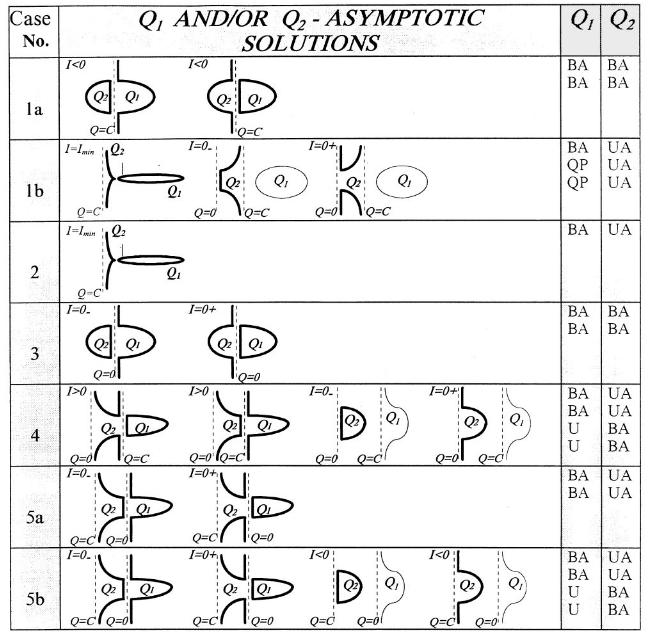

FIG. 10. The seven subcases 1: $0<C<Q_-<Q_+$ [1a: $Q_1^{(-)}<C$, 1b: $C<Q_1^{(-)}$]; 2: $C<0<Q_-<Q_+$; 3: $C<Q_-<0<Q_+$; 4: $<Q_-<C<Q_+$; 5: $Q_-<C<0<Q_+$ [5a: $Q_1^{(-)}<C$, 5b: $C<Q_1^{(-)}$] with characterization of regular (quasiperiodic or unbounded nonperiodic) states and/or asymptotic states: BA, bounded asymptotic; QP, quasiperiodic; UA, unbounded asymptotic; U, unbounded. Only in the subcases 1a and 3 do there exist pairs of bounded asymptotic solutions (solitary) for the envelopes of the interacting wave forms. The thick solid curves correspond to asymptotic states that can be bounded or unbounded. The thin solid curves correspond to regular states.

The situation is somewhat different for the remaining two subcases illustrated in Figs. 7 and 9 [subcases 4 and 5b in Eq. (37)]. Again, these subcases do not possess bounded asymptotic solutions: The bounded asymptotic state for Q_1 is accompanied by an unbounded (and nondegenerate) asymptotic one for Q_2 and vice versa, as in the three previous cases. However, one can readily observe that there exist two such combinations in each one of these subcases: For the first one (Fig. 7) two bounded-unbounded pairs for *zero* value of i (between regions α and β) and two for *positive* i (the regions α in the vicinity of $Q=C$). As far as the second one (Fig. 9) is concerned, there exist two bounded-unbounded pairs for *zero* value of i (between regions α and β in the vicinity of $Q=0$) and two for *negative* value of i (in the remaining regions β).

Figures 1, 2, and 10 provide, in a comprehensive and illustrative way, information about the possibility of launching a traveling mode (u,v) possessing a solitary (spatially or temporally localized in the moving frame) envelope of given A, B, and h. At the same time, they provide information for all the nonlinear modes whose limiting forms are all the possible asymptotic states, namely, solitary, unbounded, or degenerate. Therefore, since the basic parameters A,B are directly associated with the nonlinear shifts in frequency and wave number of the carrier (as we saw in the Introduction), the latter plays a dominant role in ''shaping-up'' the envelope (x,y).

V. CONCLUSIONS

A complete investigation of a wide class of traveling-wave solutions is made, by reducing a system of two coupled nonlinear Schrödinger (NLS) equations when it represents the so-called Manakov system, in a dynamical system that admits soliton solutions. The reduced system is a two-dimensional Hamiltonian one, which describes the motion of two coupled quartic anharmonic oscillators. This dynamical system is integrable, exhibiting one additional integral besides the Hamiltonian, which can be explicitly written even without knowing the solutions in closed form.

The reduced Hamiltonian system is shown to be separable in the Stäckel sense by transforming it to a new coordinate system (Q,P). The utilization of the Stäckel's theorem allowed us to find the solutions, involving hyperelliptic integrals. Series expressions of the latter in closed form in terms of the three elliptic integrals were given on the basis of a limited number of parameters and the initial conditions. Among these solutions, there exist several that correspond to solitary-type envelope solutions to the Manakov system.

The existence of two integrals of motion facilitated a thorough study of the system: The structure of the phase space was completely understood by investigating the expression of the second integral for a given arithmetic value of the first integral and using a Poincaré surface of sections. We noticed that the arithmetic value of the first invariant, namely the Hamiltonian, depends upon the particular choice of envelope, namely on the set of values $(x,dx/ds,y,dy/ds)$ at a reference value of the traveling-wave coordinate s and the type of the traveling waves to which one is aiming, which, in turn, relates to the spectral energy density variations of the interacting wave forms. On the other hand, the mere existence of the second integral implies that there exists an invariant relationship between the envelope amplitudes and their respective rate of change (with s).

For any given set of values for the parameters of the system, the position of the fixed points (representing periodic orbits) as well as their stability character were easily determined. This is important since the existence of fixed points is directly associated with the periodic character of the envelope of the traveling-wave solutions to the Manakov system. Special emphasis was given to the hyperbolic ones since they directly correspond to a solitary type of envelope structure. The asymptotic curves (the separatrices that correspond to the hyperbolic fixed points) defining several regions in the permissible ''area of motion'' in the phase space were thus also identified. Therefore, different types of motion associated with different sets of initial conditions and especially various quasiperiodic modes (or trajectories, in the nomenclature for the dynamical systems) of the Manakov system were completely identified within these regions. The asymptotic behavior of these trajectories was thoroughly studied since the asymptotic states correspond to the separatrices in the phase space. All possible asymptotic states were easily identified (namely, solitary, unbounded, or degenerate) whose character depended upon the behavior and value of the second invariant (integral of motion). They were also categorized and presented in a systematic way in a three-dimensional parameter space spanned by A, B, and h. The choice of parameters was based on the fact that A,B are associated with the nonlinear shifts in frequency and wave number of the carrier directly, which, in turn, are related to the initial information content of the two interacting modes that the Manakov system models while the value of h (complicated invariant dynamical function) reflects the spectral energy content carried by the interacting modes. A basic outcome of this description is the following: For given values of the parameters (A, B, and h) a (Q_1,P_1) invariant curve (on its respective Poincaré surface of section) is confined inside a subregion, corresponding to a particular value, i, of the second invariant. Simultaneously, the respective (Q_2,P_2) invariant curve with the *same value (i) of the second invariant* is confined in a subdomain that corresponds to a complementary subdomain [i.e., the same A, B, h, and i but of a (disjointedly) different set of initial conditions] on the (Q_1,P_1) Poincaré surface of section.

Finally, as far as future investigations are concerned, this work will be the basis of dynamically studying the general nonintegrable case $(\sigma\neq 1)$, which is expected to exhibit chaotic behavior as well. Furthermore, the physical meaning of the unbounded solutions, as well as the magnitude of the traveling-wave coordinate scales in Eq. (1) as compared with the scales of evolution of the particular physical system in hand, is an open question. These studies are currently in progress.

ACKNOWLEDGMENTS

This work has been supported in part by the Commission of the European Union (HCM) Network on Nonlinear Phenomena in Microphysics of Collisionless Plasmas, and in part by the General Secretariat of Research and Technology (Greek Ministry of Development) under Contracts Nos. PENED-91-ED-177, PENED-95/3312-644, and PENED-95/1242. Constructive discussions with Professor Tito J. Mendonça and Professor Felipe Romeiras of the Instituto Superior Tecnico (Lisbon, Portugal) are kindly acknowledged.

APPENDIX

The integrals involved in Eq. (27) contain a fourth-order polynomial under the square root sign in the denominator. It is well known [45] that, if the numerator is an integer power of the integration variable, integrals with such denominators can always be expressed through recurrence relations in terms of the three elliptic integrals (first, second, and third kind). The numerator at hand is the square root of the integration variable. One can always find a transformation of the integration variable that leads to a numerator of the form $(1-x)^{1/2}$ with $|x|\leqslant 1$ (the denominator transforms to a new fourth-order polynomial under the square root sign). Then

$(1-x)^{1/2}$ can be expressed in terms of a converging series of powers of the new integration argument. Therefore, one can then make use of the aforementioned property of integrals with such numerators.

This approach has been followed in calculating the hyperelliptic integrals involved in Eq. (27). After a straightforward, though lengthy, calculation, one obtains the following recurrence relation:

$$I_m^{(\gamma)}(x)=\frac{2x\left(\sum_{n=0}^{n=3}a_n^{(\gamma)}x^{4-n}\right)^{1/m-3}-\sum_{n=1}^{n=3}a_n^{(\gamma)}[2(m-1)-n]I_{m-n}^{(\gamma)}(x)}{2a_0^{(\gamma)}(m-1)}, \tag{A1}$$

where

$$a_0^{(1)}=\frac{1/2C-h}{C^2},\quad a_1^{(1)}=1+\frac{A}{C}+\frac{h}{C^2},\quad a_2^{(1)}=-\frac{A}{C},\quad a_3^{(1)}=-1, \tag{A2a}$$

$$a_0^{(2)}=\frac{i}{2C^3},\quad a_1^{(2)}=\frac{A}{C}+\frac{h}{C^2},\quad a_2^{(2)}=\frac{A}{C}-1,\ a_3^{(2)}=-1, \tag{A2b}$$

$$a_0^{(3)}=1,\quad a_1^{(3)}=-\frac{A}{C}-2,\quad a_2^{(3)}=1+\frac{A}{C}-\frac{h}{C^2},\quad a_3^{(3)}=\frac{h-i/2C}{C^2}, \tag{A2c}$$

$$A_0^{(4)}=-\frac{i}{2C^3},\quad a_1^{(4)}=\frac{A}{C}+\frac{h}{C^2},\quad a_2^{(4)}=1-\frac{A}{C},\quad a_3^{(4)}=-1, \tag{A2d}$$

$$a_0^{(5)}=-1,\quad a_1^{(5)}=2+\frac{A}{C},\quad a_2^{(5)}=-1-\frac{A}{C}+\frac{h}{C^2},\quad a_3^{(5)}=\frac{i/2C-h}{C^2}. \tag{A2e}$$

The arguments x of the functions $I_m^{(\gamma)}(x)$ are $(1-Q/C)^{-1}$, $-C/Q$, $1-Q/C$, C/Q, and $1-Q/C$, respectively, for $\gamma=1,2,...,5$. The requirements on Q's in these arguments in order to ensure convergence of the series expansion of the numerator of the integrants in Eq. (27) are, respectively, $(C<0<Q,-Q/C<1)$, $(C<0<Q,1<-Q/C)$, $(C<Q<0)$, $(0<C<Q)$, and $(0<Q<C)$, where Q may either be Q_1 or Q_2. Since the domains of variation of Q's are restricted by Eq. (11), one can easily observe that the possible combinations of functions for Q_1 and Q_2 are two: (a) types $I_m^{(1)}(x)$ or $I_m^{(2)}(x)$ for Q_1 combined with type $I_m^{(3)}(x)$ for Q_2; (b) type $I_m^{(4)}(x)$ for Q_1 combined with type $I_m^{(5)}(x)$ for Q_2. Therefore, the integral in Eq. (27) can be expressed as a series of these functions in three different ways depending upon the domain of variation of the variable $Q_1(t)$ [and the reference value $Q_1(t_0)$], namely, (i) $C<0$ and $1\geqslant -Q_1(t)/C$; (ii) $C<0$ and $-Q_1(t)/C\geqslant 1$; (iii) $C>0$.

[1] B. K. Som, M. R. Gupta, and B. Dasgupta, Phys. Lett. **72A**, 111 (1979).
[2] J. C. Bhakta, Plasma Phys. Controlled Fusion **29**, 245 (1987).
[3] M. R. Gupta, B. K. Som, and B. Dasgupta, J. Plasma Phys. **25**, 499 (1981).
[4] A. Hasegawa and F. Tappert, Appl. Phys. Lett. **23**, 142 (1973).
[5] B. Crosignani and P. Di Porto, Opt. Lett. **6**, 329 (1981).
[6] S. M. Jensen, IEEE J. Quantum Electron. **QE-18**, 1580 (1982).
[7] Y. Silberberg and G. I. Stegeman, Appl. Phys. Lett. **50**, 801 (1987).
[8] C. R. Menyuk, IEEE J. Quantum Electron. **QE-23**, 174 (1987).
[9] C. R. Menyuk, Opt. Lett. **12**, 614 (1987).
[10] C. R. Menyuk, IEEE J. Quantum Electron. **QE-25**, 2674 (1989).
[11] H. G. Winful, Appl. Phys. Lett. **47**, 213 (1985).
[12] S. Trillo, S. Wabnitz, E. M. Wright, and G. I. Stegeman, Opt. Commun. **70**, 166 (1989).
[13] S. V. Manakov, Zh. Eksp. Teor. Fiz. **65**, 505 (1973) [Sov. Phys. JETP **38**, 248 (1974)].
[14] V. E. Zakharov and E. I. Schulman, Physica D **4**, 270 (1982).
[15] D. J. Kaup and B. A. Molomed, Phys. Rev. A **48**, 599 (1993).
[16] G. I. Stegeman and E. M. Wright, Opt. Quantum Electron. **22**, 95 (1990).
[17] C. Elphick, J. Phys. A **16**, 4013 (1983).
[18] P. A. Belanger and C. Paré, Phys. Rev. A **41**, 5254 (1990).
[19] D. N. Christodoulides and R. I. Joseph, Opt. Lett. **13**, 53 (1988).
[20] Yu. S. Kivshar, Opt. Lett. **18**, 337 (1993).
[21] C. Paré and M. Florjanczak, Phys. Rev. A **41**, 6287 (1990).
[22] T. Ueda and W. L. Kath, Phys. Rev. A **42**, 563 (1991).
[23] C. R. Menyuk, Opt. Lett. **12**, 614 (1987).
[24] C. R. Menyuk, J. Opt. Soc. Am. B **5**, 392 (1988).
[25] E. M. Wright, G. I. Stegeman, and S. Wabnitz, Phys. Rev. A **40**, 4455 (1989).

[26] Yu. S. Kivshar, J. Opt. Soc. Am. B **7**, 2204 (1990).
[27] S. Trillo, S. Wabnitz, E. M. Wright, and G. I. Stegeman, Opt. Lett. **13**, 871 (1988).
[28] M. N. Islam, C. D. Poole, and J. P. Gordon, Opt. Lett. **14**, 1011 (1989).
[29] C. Z. J. Chen, P. K. A. Wai, and C. R. Menyuk, Opt. Lett. **15**, 477 (1990).
[30] B. A. Malomed and S. Wabnitz, Opt. Lett. **16**, 1388 (1991).
[31] P. S. Tasgal and M. J. Potasek, J. Math. Phys. **33**, 1208 (1992).
[32] V. M. Eleononskii, V. G. Korolev, N. E. Kulagin, and L. P. Shil'nikov, Zh. Eksp. Teor. Fiz. **99**, 1113 (1991) [Sov. Phys. JETP **72**, 619 (1991)].
[33] M. Haelteman, A. P. Sheppard, and A. W. Snyder, Opt. Lett. **18**, 1406 (1993).
[34] M. Haelterman and A. P. Sheppard, Phys. Rev. E **49**, 3376 (1994).
[35] D. V. Choodnovsky and G. V. Choodnosky, Lett. Nuovo Cimento **22**, 47 (1978).
[36] J. Hietarinta, Phys. Rep. **147**, 87 (1987).
[37] P. Stäckel, Math. Ann. **35**, 91 (1890).
[38] P. Stäckel, Math. Ann. **42**, 537 (1893).
[39] P. Stäckel, Z. Reine Angew. Math. **128**, 222 (1912).
[40] J. L. Bishop, Astrophys. J. **322**, 618 (1987).
[41] P. T. de Zeeuw and C. Hunter, Astrophys. J. **356**, 365 (1990).
[42] D. J. Frantzeskakis, K. Hizanidis, G. S. Tombras, and I. Belia, IEEE J. Quantum Electron. **QE-31**, 183 (1995).
[43] M. V. Tratnik and J. E. Sipe, Phys. Rev. A **38**, 2011 (1988).
[44] M. Lakshamanan and R. Sahadenvan, Phys. Rev. A **31**, 861 (1985).
[45] H. Hancock, *Lectures on the Theory of Elliptic Functions* (Dover, New York, 1958).
[46] G. Contopoulos, Astrophys. J. **153**, 83 (1968).
[47] E. Infeld and G. Rowlands, *Nonlinear Waves, Solitons and Chaos* (Cambridge University Press, Cambridge, 1990).